ISBN: 978-3-95450-227-1 ISSN: 2673-5490 doi:10.18429/JACoW-IPAC2022-WEPOPT042

DESIGNING THE EIC ELECTRON STORAGE RING LATTICE FOR A WIDE ENERGY RANGE*

D. Marx†, J.S. Berg, J. Kewisch, Y. Li, C. Montag, V. Ptitsyn, S. Tepikian, F. Willeke, D. Xu, Brookhaven National Laboratory, Upton, NY, USA
G.H. Hoffstaetter, D. Sagan, M.G. Signorelli, J. Unger, Cornell University, Ithaca, NY, USA
V. Morozov, Oak Ridge National Laboratory, Oak Ridge, TN, USA
Y. Cai, Y. Nosochkov, SLAC, Menlo Park, CA, USA
B.R.P. Gamage, Thomas Jefferson National Accelerator Facility, Newport News, VA, USA

Abstract

The Electron-Ion Collider (EIC) will collide electrons with hadrons at center-of-mass energies up to 140 GeV (in the case of electron-proton collisions). A 3.8-kilometer electron storage ring is being designed, which will store electrons with a range of energies up to 18 GeV for collisions at one or two interaction points. At energies up to 10 GeV the arcs will be tuned to provide 60 degree phase advance per cell in both planes, whereas at top energy of 18 GeV a 90 degree phase advance per cell will be used, which largely compensates for the horizontal emittance increase with energy. The optics must be matched at three separate energies, and the different phase-advance requirements in both the arc cells and the straight sections make this challenging. Moreover, the spin rotators must fulfill requirements for polarization and spin matching at widely different energies while satisfying technical constraints. In this paper these challenges and proposed solutions are presented and discussed.

INTRODUCTION

The Electron-Ion Collider (EIC) [1, 2] is a new machine currently being designed that will collide polarized electrons with polarized hadrons (protons up to heavy ions) for the purpose of investigating the structure and properties of nucleons. It will be built at Brookhaven National Laboratory in the 3.8-kilometer tunnel that currently houses the Relativistic Heavy Ion Collider (RHIC) [3–5]. Two electron rings will be built in this tunnel: a rapid cycling synchrotron (RCS) [6] for accelerating electrons to collision energies and an electron storage ring (ESR) for colliding electrons with hadrons from a separate storage ring. Figure 1 shows a schematic of the EIC. Collisions will occur at a range of center-of-mass energies between 29 GeV and 140 GeV, providing luminosities up to $10^{34}\,\mathrm{cm}^{-2}\mathrm{s}^{-1}$. These luminosities are considerably greater than those achieved at HERA [5, 7], an electron/positron-proton collider that operated until 2007 at DESY, and, although the top center-of-mass energy will be less than HERA's 318 GeV, the EIC will be optimized for a much wider range of energies.

* Work supported by Brookhaven Science Associates, LLC, under Contract No. DE-SC0012704, by Jefferson Science Associates, LLC, under Contract No. DE-AC05-06OR23177, by UT-Battelle, LLC, under contract DE-AC05-00OR22725, and by SLAC under Contract No. DE-AC02-76SF00515 with the U.S. Department of Energy.
† dmarx@bnl.gov

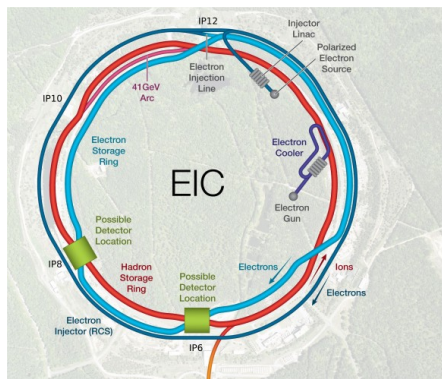

Figure 1: Schematic of EIC (not to scale).

The ESR lattice consists of six arcs with straight sections in between, labeled according to the numbers on a clock face. The baseline design for the EIC includes a single interaction point (IP), called IP6, where the beams will collide. A second IP and detector in the neighboring straight section, IP8, may be included in a future upgrade. Superconducting RF cavities will be installed at IP10, and the beam will be injected into the ring at IP12.

In order to achieve the desired range of center-of-mass energies, three values for the electron beam energy are considered: 5-6, 10, and 18 GeV. This introduces several challenges in the lattice design. As the horizontal equilibrium emittance increases with energy, this needs to be compensated to satisfy aperture requirements. Superbends in arc cells and changes to the arc phase advance are used to keep the horizontal emittance within an acceptable range. The nonlinear chromaticity correction scheme also needs to be altered for different energies, as the different arc phase advances call for different sextupole configurations.

One of the key requirements for the experimental program is a high level of longitudinal spin polarization. Beams are injected with vertical spin, which is the stable spin direction for the ring. On each side of the IPs, a solenoid-based spin rotator rotates the spin vector into or from the longitudinal direction. As the spin-rotation angles depend on energy, designing these spin rotators for operation at a wide range of energies is challenging.

Table 1 shows the main lattice parameters at different energies. In the following sections, the design challenges arising from the wide energy range are described.

ISBN: 978-3-95450-227-1 ISSN: 2673-5490 doi:10.18429/JACoW-IPAC2022-WEPOPT042

Table 1: ESR 1IP Lattice Parameters at Various Energies, the Optics Depend on Energy, and the Parameters for 5 and 10 GeV are From an Earlier Version of the Lattice

Parameter	5 GeV	10 GeV	18 GeV
Arc phase	60°	60°	90°
Superbends	On	Off	Off
Hor. emit. (nm)	26	22	27
Energy spread	0.050%	0.053%	0.095%
Tunes, Q_x/Q_y	40.12/37.1	40.12/37.1	52.12/44.1
Nat. chrom.	-80/-93	-75/-90	-93/-93

DAMPING AND EMITTANCE

The horizontal equilibrium emittance in an electron ring is given by the equation [8]

$$\epsilon_x = \frac{C_q}{J_x}\gamma^2 \frac{\langle G^3 \mathcal{H} \rangle}{\langle G^2 \rangle}, \quad (1)$$

where $C_q = 3.84 \times 10^{-13}$ m, J_x is the horizontal damping partition number, γ is the Lorentz factor, G is the inverse of the bending radius, and $\mathcal{H} = \gamma_x \eta^2 + 2\alpha_x \eta\eta' + \beta_x \eta'^2$, where $\alpha_x, \beta_x, \gamma_x$ are the Courant-Snyder parameters and η is the horizontal dispersion. The dependence on γ^2 means that the emittance would change by an order of magnitude if the same lattice were used at all energies. In order to compensate this effect, $\mathcal{H}$ may be changed by adjusting the optics of the lattice. At lower energies up to 10 GeV the phase advance in the arc cells is 60°, while at 18 GeV it is set to 90°, which largely compensates for the emittance increase with energy.

Superbends are used in the arcs, consisting of two long dipoles with a shorter one in between, as shown in Fig. 2. At energies above 10 GeV, all three magnets produce a field in the same direction with the effect of a single dipole. At lowest energy, however, the central dipole has reversed field, which produces additional damping. This allows a larger beam-beam tune shift to be supported [9], while increasing the horizontal equilibrium emittance [10, 11].

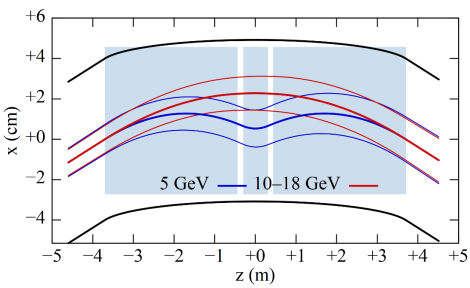

Figure 2: Illustration of superbends in the arcs at various energies. The beam envelopes shown correspond to 10σ for the 60° arc-cell phase advance.

Fine-tuning the emittance may be achieved in operation by adjusting the damping partition numbers by means of changing the frequency to produce a small radial shift [12].

SEXTUPOLE CONFIGURATION

The ESR nonlinear chromaticity correction scheme is based on multiple families of -I sextupole pairs in the arcs. One of the consequences of changing the phase advance of the arc cells is that this affects the sextupole family arrangement. The chromatic beta-beat wave propagates at twice the betatron phase advance, which means the simplest family arrangement is three families per plane at 60° arc-cell phase advance and two families per plane at 90°. The sextupole wiring scheme will be designed to allow switching between these two configurations. Chromaticity correction at 18 GeV represents the most challenging case due to the larger energy spread at higher energies, which leads to a greater momentum acceptance requirement ($10\sigma_\delta$ is required for sufficient lifetime), as well as stringent phase-advance requirements caused by using just two families of sextupoles per plane (per arc). More details on the chromaticity-correction scheme are presented in [13].

SPIN ROTATORS

Spin rotators will be located on both sides of the IP to rotate the spin vector from the vertical direction in the arcs to the longitudinal direction at the IP and back [14]. Designing spin rotators for a broad range of energies is a challenge. The lowest energies of 5 to 6 GeV preclude the use of spin rotators based purely on dipoles, as were used at HERA, due to the excessively large aperture required to accommodate orbit excursions at these energies. Instead, the spin rotators will be composed of a combination of solenoids, dipoles, and matching quadrupoles [15–17]. In general, the spin precesses around an axis parallel to the field direction, namely vertical in dipoles and longitudinal in solenoids. A solenoid followed by dipoles can therefore rotate the spin direction from vertical in the arc to radial after the solenoid, and finally to longitudinal after the dipoles. The configuration is mirror symmetric about the IP to rotate the spin from longitudinal back to vertical on the other side.

As the spin configuration needs to rotate the spin at three different energies and the dipole angles cannot be changed in operation, the solenoid-bend structure is repeated, as shown in Fig. 3, which offers the required flexibility. However, the lengths of the two solenoids, as well as the bending angles, are different in the two cases to optimize to the requirements at various energies.

Furthermore, each solenoid is actually split into two halves with a set of quadrupoles in between. This unit, collectively called a solenoid module, is shown in Fig. 4. This configuration allows decoupling between the horizontal and vertical planes, as well as horizontal spin-matching conditions, to be fulfilled. There are four superconducting half-solenoids per spin rotator: two long and two short. An alternative scheme involving skew quadrupoles outside of the half-solenoids

ISBN: 978-3-95450-227-1 ISSN: 2673-5490 doi:10.18429/JACoW-IPAC2022-WEPOPT042

was also considered and determined to be less desirable due to the added complexity in dealing with coupling from these skew quadrupoles.

The short-solenoid module sits directly next to the arc with two quadrupoles for matching in between. Between the short- and long-solenoid modules is a bending section consisting of dipoles and quadrupoles for matching. The long-solenoid module leads onto the IR section, containing quadrupoles and dipoles for matching various constraints, including a fixed dipole angle to the IP to complete the spin rotation.

Ideally zero dispersion in both short- and long-solenoid modules would be achieved by suppressing the dispersion at the end of the arcs. The challenge is matching dispersion in as few arc cells as possible, which is necessary because changes in the β and dispersion functions will ruin the sextupole pairing. Previous studies showed that pairing the sextupoles is particularly important for maximizing the dynamic aperture of the 90° lattice. For this reason the preferred solution is to leave the 90° arcs unchanged to the end and to bring the dispersion down in the short-solenoid module and bend module. The dispersion is then zero in the long-solenoid module. The implication of this scheme is that the short solenoids have to be turned off at top energy, which does not allow full longitudinal spin matching.

At intermediate energy of around 10 GeV and lower, the phase advance of the arc FODO cells is 60°, and the short solenoids must be turned on. It would require very large strengths to match the dispersion and its derivative to zero by varying only two quadrupoles, although it can be done with reasonable strengths if all quadrupoles in the last two arc cells are used. As a compromise, it was decided to vary only the quadrupoles in the last arc cell, which is sufficient to lower the dispersion to less than about 0.2 m in the short-solenoid module. The bend section between the solenoid modules can then be used to bring down the dispersion to zero in the long-solenoid module.

The bend angles must be set to provide the required spin rotation at all energies. The spin rotates in a dipole with bend angle θ by $\psi = a\gamma\theta$ with respect to the beam axis, where a is the anomalous magnetic moment of an electron [15]. The dipoles between the end of the spin rotator and the IP must rotate the spin vector by a full $\pi/2$ angle at the maximum energy of 18 GeV, as only the long solenoids are turned on, which requires a bending angle of 38.79 mrad. At minimum energy, the total bend angle from the beginning of the spin rotator to the IP should result in a $\pi/2$ rotation. This would

Figure 3: The spin rotators are composed of short- and long-solenoid modules, as well as bend modules, to rotate the spin from vertical in the arcs to longitudinal at the IP and back to vertical on the other side.

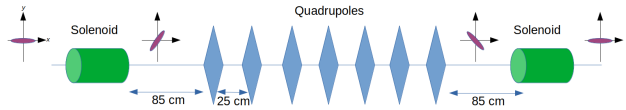

Figure 4: Each solenoid module consists of two half-solenoids with five or seven quadrupoles in between.

result in a 97.81 mrad bend angle between the solenoid modules at the nominal minimum energy of 5 GeV. At an energy of 6 GeV, this angle is reduced to 77.57 mrad. The current lattice has this latter bend angle, and 6 GeV is taken as the minimum energy, while a study is ongoing to assess the feasibility of adjusting the geometry to achieve longitudinal polarization down to 5 GeV. The total bend angle is repeated in all the other straight sections for symmetry reasons.

The spin-rotation angle in a solenoid is related to its length, L, and strength, K_s, by $\phi = (1 + a)K_sL$ [14]. At top and bottom energies, only one solenoid module is used, which must provide $\pi/2$ spin rotation, whereas at 10 GeV both are used to rotate the spin, with the spin-rotation angles shown in Table 2. The energies have been adjusted slightly to ensure half-integer spin tunes ($a\gamma$).

Table 2: Solenoid Module Spin-rotation Angles at Various Energies, ϕ_1 is the Angle Between the Short- and Long-solenoid Modules, and ϕ_2 is the Angle Between the Long-solenoid Module and IP

Energy (GeV)	ϕ_1 (rad)	ϕ_2 (rad)
17.846	0	$\pi/2$
9.915	0.7111	1.7193
5.949	$\pi/2$	0

Matching the solenoid modules to achieve decoupling and horizontal spin matching by optimizing the quadrupole strengths is a key challenge described in [14].

IR MATCHING

Optimizing the beam-beam interaction at different energies results in different required β^* parameters [18]. They depend on both the electron and hadron energies. In addition, the detector solenoid strength does not scale with energy, so its effect will be particularly significant at lower energies and will require compensation [19].

CONCLUSION

The ESR is designed to operate at a large range of energies. There are many physical effects, such as radiation, spin polarization, and beam-beam interactions, that mean that a simple scaling of the magnet strengths is not sufficient. Instead, the lattice design at different energies is radically different, with different cell phase advances, superbend settings, sextupole configurations, spin-rotator settings, and β^* parameters. Significant progress has been made in the lattice design at various energies, in particular the spin-rotator design, which is still evolving. In the future, the possibility of achieving longitudinal spin polarization at 5 GeV energy will be studied.

ISBN: 978-3-95450-227-1 ISSN: 2673-5490 doi:10.18429/JACoW-IPAC2022-WEPOPT042

REFERENCES

[1] J. Beebe-Wang *et al.*, "Electron-Ion Collider: Conceptual Design Report," Brookhaven National Laboratory, Jefferson Lab, 2021, www.bnl.gov/EC/files/EIC_CDR_Final.pdf

[2] C. Montag *et al.*, "Electron-Ion Collider Design Status," presented at IPAC'22, Bangkok, Thailand, Jun. 2022, paper WEPOPT044, this conference.

[3] C. Montag, "RHIC status and plans," *AIP Conference Proceedings*, vol. 2160, no. 1, p. 040 006, 2019, doi:10.1063/1.5127686

[4] "RHIC Configuration Manual," Brookhaven National Laboratory, 2006, www.bnl.gov/cad/accelerator/docs/pdf/RHICConfManual.pdf

[5] K. Hübner *et al.*, "The largest accelerators and colliders of their time," in *Particle Physics Reference Library : Volume 3: Accelerators and Colliders*, 2020, doi:10.1007/978-3-030-34245-6_10

[6] V. H. Ranjbar, H. L. III, F. Meot, and F. Lin, "EIC's Rapid Cycling Synchrotron Spin Tracking Update," presented at IPAC'22, Bangkok, Thailand, Jun. 2022, paper THPOST004, this conference.

[7] "An Assessment of U.S.-Based Electron-Ion Collider Science," National Academies of Sciences, 2018, ch. 5 Comparison of a U.S.-Based Electron-Ion Collider to Current and Future Facilities, doi:10.17226/25171

[8] S. Peggs and T. Satogata, *Introduction to Accelerator Dynamics*. Cambridge University Press, 2017, doi:10.1017/9781316459300

[9] G. Guignard, "Beam-beam limit as a function of the damping time in electron rings," *IEEE Transactions on Nuclear Science*, vol. 28, no. 3, pp. 2506–2508, 1981, doi:10.1109/TNS.1981.4331738

[10] Robin, D. Nishimura, and Hiroshi, "Impact of Superbends at the ALS," in *Proc. PAC'99*, New York, NY, USA, Mar. 1999, https://jacow.org/p99/papers/TUCL5.pdf

[11] D. Robin, "Superbend Upgrade at the Advanced Light Source," in *Proc. PAC'03*, Portland, OR, USA, May 2003, https://jacow.org/p03/papers/TOPA002.pdf

[12] M. G. Minty, R. Akre, F. J. Decker, J. Frisch, S. Kuroda, and F. Zimmermann, "Emittance reduction via dynamic RF frequency shift at the SLC damping rings," in *Proc. 17th International Conference on High Energy Accelerators (HEACC'98)*, Dubna, Russia, 1998.

[13] Y. M. Nosochkov *et al.*, "Dynamic Aperture of the EIC Electron Storage Ring," presented at IPAC'22, Bangkok, Thailand, Jun. 2022, paper WEPOPT043, this conference.

[14] D. Marx *et al.*, "Task Force Report: ESR Linear Lattice Design," Brookhaven National Laboratory, BNL-222485-2021-TECH, EIC-ADD-TN-025, 2021, https://technotes.bnl.gov/PDF?publicationId=222485

[15] D. Barber *et al.*, "A solenoid spin rotator for large electron storage rings," *Particle Accelerators*, vol. 17, pp. 243–262, 1985.

[16] P. Emma, "A spin rotator system for the nlc," SLAC, 1994.

[17] V. Ptitsin and Y. Shatunov, "Siberian Snakes for Electron Storage Rings," in *Proc. PAC'97*, Vancouver, Canada, May 1997.

[18] J. Qiang, Y. Luo, C. Montag, F. J. Willeke, D. Xu, and Y. Hao, "Strong-Strong Simulations of Coherent Beam-Beam Effects in the EIC," presented at IPAC'22, Bangkok, Thailand, Jun. 2022, paper WEPOPT041, this conference.

[19] D. Xu and F. J. Willeke, "EIC Beam Dynamics Challenges," presented at IPAC'22, Bangkok, Thailand, Jun. 2022, paper WEIXGD1, this conference.